 DOI: 10.3217/978-3-85125-528-7-08

3-D Shape Recovery of the Left Heart Chamber from Biplane X-Ray Projections Using Anatomical A-Priori Information Learned from CT

Roland Swoboda[1,2], Josef Scharinger[2], and Clemens Steinwender[3]

[1] Research Center Hagenberg
University of Applied Sciences Upper Austria, Austria
roland.swoboda@fh-hagenberg.at

[2] Department of Computational Perception
Johannes Kepler University Linz, Austria
josef.scharinger@jku.at

[3] Clinic of Internal Medicine I
General Hospital Linz, Austria
clemens.steinwender@akh.linz.at

Abstract

Recovering the 3-D shape of the left heart chamber from bi-planar 2-D x-ray projection images is a challenging task since only sparse and noisy data is available for reconstruction. In this work, a 3-D statistical shape model (SSM) of the left ventricular (LV) anatomy is learned from high-resolution CT data and utilized as a-priori information to solve the under-determined and ambiguous reconstruction problem. A 2-D/3-D registration method fits the SSM to the x-ray images of the patient by calculating simulated projections of the SSM and minimizing the difference between simulated and given projections. The presented approach is evaluated using simulated and real patient data. For patients where both projection images and CT data are available, the reconstructed LV is compared to the true shape known from CT. Our results show a good correspondence between recovered and true shapes. Using a SSM as anatomical a-priori information for reconstruction helps in limiting the space of possible solutions and allows to generate statistically plausible shapes.

1. Introduction

Cardiac diseases are one of the most common causes of death in the industrialized world today. In the case of acute myocardial infarction, for instance, interventional x-ray angiography is state-of-the-art for both treatment and diagnosis. To evaluate the viability of myocardium after infarction, a catheter is advanced into the left heart chamber (ventricle) and contrast agent is injected to opacify the ventricular cavity during radiation. Bi-planar cine-angiographic equipment is used to acquire two x-ray image sequences simultaneously from standard right anterior oblique (RAO) and left anterior oblique (LAO) views, see Fig. 1.

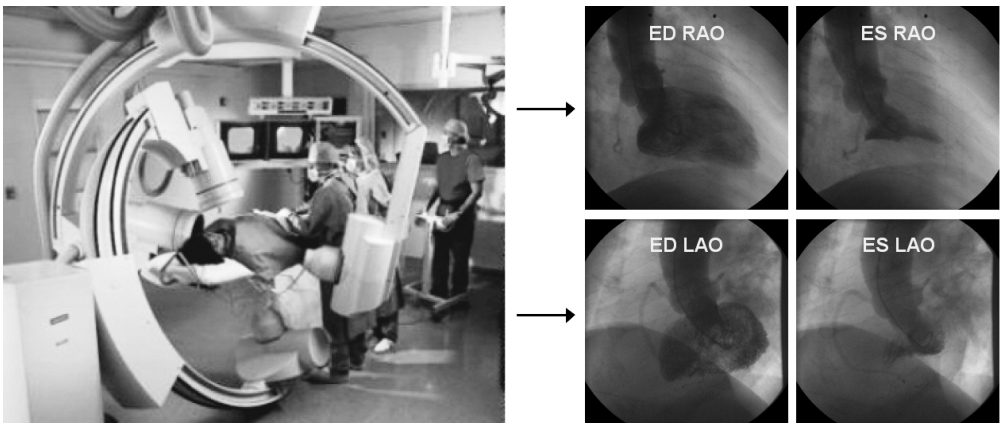

Figure 1. Biplane cine-angiographic x-ray equipment used in the catheter lab to acquire images for quantitative left ventricle analysis.

The gold standard for quantitative left ventricle analysis in the catheter lab is based on the evaluation of end-diastolic (ED) and end-systolic (ES) endocardial contour information gathered from these 2-D projection images. The ED and the ES volume are calculated (by applying e.g. the Area-Length method) and used to determine ejection fraction (EF), i.e. the volume that is squeezed out during contraction. Contour information is further utilized by wall motion analysis methods (like e.g. the Centerline method) to quantify myocardial viability. However, since 3-D information is lost due to projection, volumetric diagnostic parameters, like EF, can only be approximated and wall motion is only evaluable for LV surface areas with the boundary visible in the projection image. Novel approaches aim at reconstructing the spatio-temporal shape of the LV to perform analysis in 3-D [10].

2. Related Work

In classical computed tomography (CT), hundreds of projections are acquired by a fast rotating x-ray gantry. Analytical and algebraic reconstruction techniques exploit this dense information to yield voxel values that vary within a continuous range. However, these techniques typically fail if merely two (noisy) projections are available. C-arm CT is a relatively young and hybrid type of imaging modality, where the C-arm is rotated during acquisition to increase the number of projections. Techniques known from CT can then be utilized to address the reconstruction problem [8]. In the catheter lab, however, the application of C-arm CT is challenged by the higher amount of x-ray dose and bolus compared with conventional x-ray angiography (XA), and the slower rotational speed of the C-arm compared with classical CT when imaging the rapidly moving heart. Whether C-arm CT will substitute XA as a routine method in future remains to be seen [9].

Unlike classical (continuous) CT, discrete tomography focuses on reconstruction problems where only a small number of projections – as small as two – are available and the object's intensity levels are limited, i.e. discrete, and known a-priori [3]. Using additional a-priori information is crucial when trying to solve such under-determined and ambiguous problems, since this can reduce the space of possible solutions and improve the ability to deal with noisy projection data. Some of the early approaches published in the field of 3-D LV shape recovery from XA rely on the assumption that ventricular cross-sections follow certain geometric priors (like connectedness, convexity, symmetry, roundness, etc.), however, this is usually too restrictive in practice. In the work of Prause and Onnasch [7], digitized post-mortem human LV casts are used as a-priori information. Other approaches often do not incorporate anatomical a-priori information at all [5], [6].

The novelty of our approach is that anatomical a-priori information is learned from high-resolution CT data and modeled as a SSM, which is then fit to the angiograms by a 2-D/3-D registration method. The application of SSMs for recovering shape from angiography has been successfully demonstrated by other authors for hard-tissue objects like the pelvis [4] or the vertebrae [1], but not yet for non-rigid contrast-enhanced soft-tissue objects like the LV. This paper is a refinement of our previous work [12]. For the sake of comprehensibility, parts of Sec. 3 and 4 are based thereon.

3. Methods

3.1. Statistical Shape Models

In order to build a 3-D SSM [2], a set of segmentations of the target shape is required. The contour of each shape S_i is described by n landmarks, i.e. points of correspondence that match between shapes, and represented as a vector of coordinates: $x_i = (x_1, ..., x_n, y_1, ..., y_n, z_1, ..., z_n)_i^T$. All n_s shape vectors form a distribution in a $3n$-dimensional space. This distribution is approximated by $x = \bar{x} + \Phi b$, with $\bar{x} = \frac{1}{n_s} \sum_{i=1}^{n_s} x_i$ being the mean shape vector and b being the shape parameter vector. By varying b, new instances of the shape class are generated. Φ is obtained by performing a principal component analysis (PCA) on the covariance matrix $C = \frac{1}{n_s - 1} \sum_{i=1}^{n_s} (x_i - \bar{x})(x_i - \bar{x})^T$. PCA yields the principal axes of this distribution; the eigenvalues give the variances of the data in the direction of the axes (= eigenvectors). To reduce noise and dimensionality only those eigenvectors with the largest t eigenvalues are used. t denotes the number of the most significant modes of variation (MOV) and is chosen so that a fraction f of the total variation is retained, $\sum_{j=1}^{t} \lambda_j \geq f \sum \lambda_j$. Prior to statistical analysis, location, scale and rotational effects must be removed from the training shapes to obtain a compact model. Commonly, Procrustes analysis is applied to minimize $D = \sum |x_i - \bar{x}|^2$, the sum of squared distances (SSD) of each shape to the mean.

3.2. Modeling of Anatomical A-Priori Information

A Siemens Somatom Sensation Cardiac 64 multi-slice CT is used to acquire 20 data sets at 65% of the heart phase (R-R peaks) with an effective slice thickness of 0.5 mm and an average in-plane resolution of 0.33 mm. The size of the image mask in the transversal plane is 512×512 pixels; the number of slices varies between 220 and 310. The endocardial LV surface is manually segmented by experts in cardiology. Contours are specified in each fifth axial slice by interactively setting control points of a cardinal spline; intermediate contours are interpolated. The surface of an LV is represented as a stack of contours. Details like the atrial concavity, the apex and the aortic valve region are retained during segmentation to obtain an accurate model of the anatomy. Point correspondence among the training shapes is established based on back-propagation of the landmarks on a mean shape [11]. After segmentation, landmark extraction and removing location, scale and rotational effects, the SSM is built as outlined in Sec. 3.1. The first three MOV of the final model are illustrated in Fig. 2.

3.3. Left Ventricular Shape Recovery

In discrete tomography, a common strategy for solving the under-determined and ambiguous reconstruction problem is to use numeric optimization [3]. As an exact solution will usually not be available, the projections of the recovered object need only be approximately equal to the given projection data. In this work, a 2-D/3-D registration approach is followed to minimize the difference between the given projections and the simulated projections derived from the SSM. To transform the SSM from

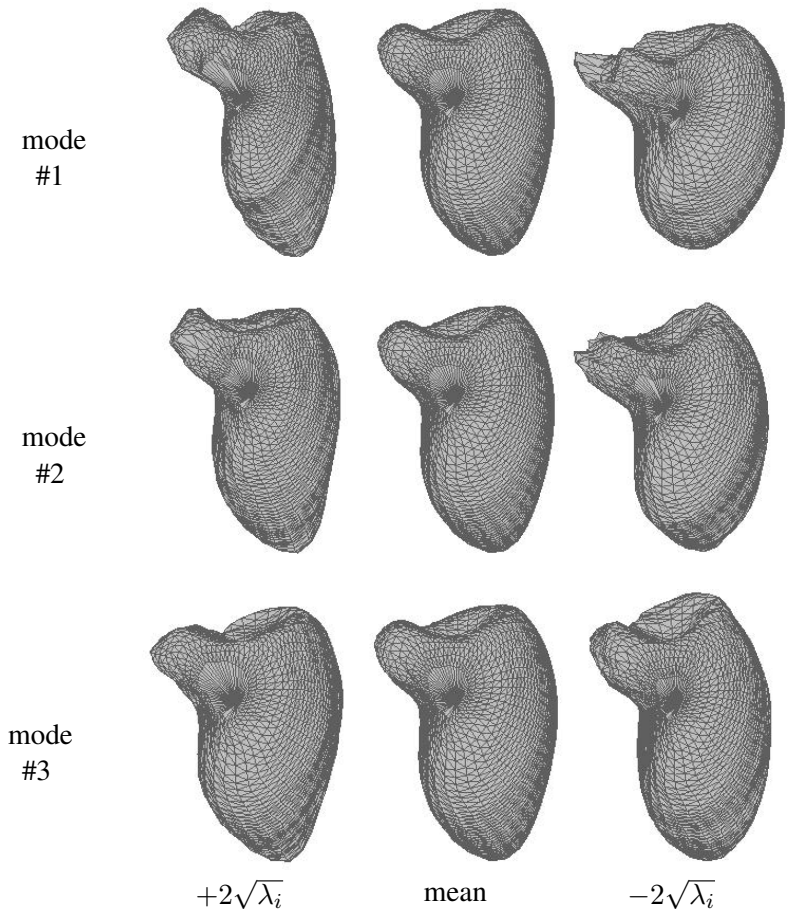

Figure 2. First three modes of variation of the LV SSM.

model space to image space the following equation is used: $y = R\left((\bar{x} + \Phi b)\, s + T\right)$. Both shape parameter vector b and the parameters for pose $p = \{R, s, T\}$, i.e. rotation matrix R, scale factor s and translation vector T, have to be found so that the registration error is minimized. Unlike [4] and [1], we derive R from Euler angles to reduce the dimensionality of the registration problem. Orientation in 3-D space is thus described using 3 angles, i.e. $R_{\alpha,\beta,\gamma}$, instead of a 3×3 matrix. To generate statistically plausible shapes [2], b is constrained by $\pm 2\sqrt{\lambda_i}$. In contrast to [4] and [1], we exploit the training data to derive constraints for p. The training instances in model space are transformed to image space and the range of the pose vector components is analyzed. Note that this can be regarded as additional a-priori information. To minimize our cost function, the Nelder-Mead algorithm is applied. Experiments showed that optimizing pose and shape sequentially is more efficient than optimizing both simultaneously.

3.3.1. Cost Function

Our cost function depends on the shape and the pose parameter vector and incorporates both contour and densitometric information derived from the given projections P_i and the simulated projections $P_i'(b,p)$: $\epsilon(b,p) = \sum_{i=1}^{n_P} \left(\omega_C \epsilon_C(P_i, P_i'(b,p)) + \omega_D \epsilon_D(P_i, P_i'(b,p))\right)$. Contour-related error ϵ_C is obtained by equiangular sampling of the given and the simulated contour and by calculating the SSD for the sampled points. As density-related error ϵ_D, the sum of squared difference metric is used. Total error ϵ is defined as the weighted sum of ϵ_C and ϵ_D over all $n_P = 2$ projections.

3.3.2. Extraction of Contour and Densitometric Information

In the case of in-vivo angiograms, the endocardial contour is segmented by experts in cardiology prior to reconstruction. Densitometric information is derived by means of digital subtraction angiography. From the initial frames of an angiographic sequence showing no contrast agent, a mask is deduced. Logarithmic subtraction of mask and current frame is performed due to the exponential attenuation of x-rays. To reduce noise and the inhomogeneous saturation of contrast agent within the ventricle, two frames before and after a frame are used for averaging. In the case of simulated angiograms, contour information is extracted by border detection, whereas densitometric information is measured directly.

3.4. Simulation of Angiographic Projections

Both the presented reconstruction approach and the following evaluation strategy require the simulation of projections. Our model of the bi-planar angiographic device calculates the exact position of the x-ray sources and the image intensifier planes for the projections. For a given viewing direction, shape and pose parameter vector, a simulated projection of the SSM in image space is obtained in two steps. First, the polygonal model is converted into a 3-D binary image, V, whose values denote the presence/absence of contrast agent. Then, a projection is derived using ray-casting. Since densitometric information is expected to be linear for reconstruction, an exponential attenuation of x-rays has not been incorporated into the simulation process.

4. Results

The presented methods are implemented and evaluated using Matlab and the Image Segmentation and Registration Toolkit (ITK) C++ library. To quantify the difference between original and recovered shape, two geometric and three volumetric similarity metrics are defined for comparing the polygonal models and the binary image representations, respectively. An exemplary reconstruction result of the performed leave-one-out experiments is illustrated in Fig. 3.

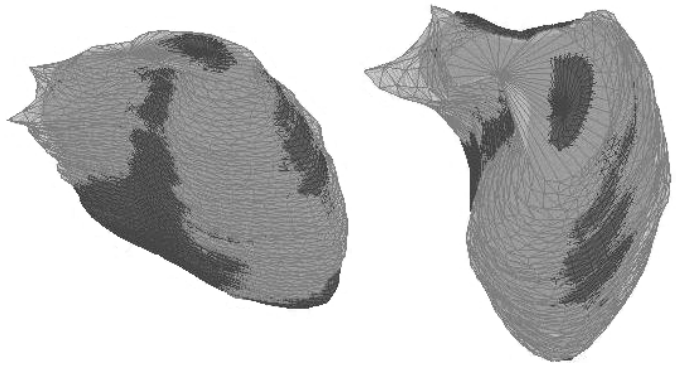

Figure 3. Reconstruction example showing original shape (bright) and recovered shape (dark).

4.1. Similarity Metrics

Similarity of two polygonal models S_1 and S_2 is measured based on a given distance metric d: $sim_d(S_1, S_2) = \frac{1}{2}(\frac{1}{n}\sum_{i=1}^{n} d(p_i, S_2) + \frac{1}{m}\sum_{j=1}^{m} d(q_j, S_1))$, $p_{i=1,\ldots,n} \in S_1, q_{j=1,\ldots,m} \in S_2$. Distance metric d_{min} is defined as the Euclidean distance between point p_i and its closest point on S_2: $d_{min}(p_i, S_2) =$

$\min_{q_j \in S_2} |p_i - q_j|$. Distance metric d_{ortho} denotes the Euclidean distance between p_i and the point obtained by intersecting S_2 with the surface normal at p_i: $d_{ortho}(p_i, S_2) = |p_i - \mathrm{surfn}(p_i) \cap S_2|$.

Let $|V|$ denote the volume of a 3-D binary image V. Volume conformity is measured by calculating the difference of volumes (DOV): $sim_{DOV} = 1 - abs(|V_{orig}| - |V_{rec}|)/|V_{orig}|$. To assess shape conformity, the volume of differences (VOD) metric is used: $sim_{VOD} = 1 - |\mathrm{xor}(V_{orig}, V_{rec})|/|V_{orig}|$. An alternative metric for shape conformity, derived from kappa statistic, quantifies the overlap between two binary masks: $sim_{\kappa} = 2|V_1 \cup V_2|/(|V_1| + |V_2|)$.

4.2. Evaluation based on Simulated Data

Evaluation with simulated data is performed based on leave-one-out experiments. From the 20 segmented CT data sets, all but one are used to learn a SSM. Simulated angiograms from RAO and LAO view are calculated for the left-out data set as described in Sec. 3.4, and from these angiograms shape is recovered by fitting the learned SSM. The recovered shape is compared with the segmented shape of the left-out data set using the defined similarity metrics. This procedure is repeated for each data set. The DOV metric in Tab. 1 shows that the original volume is approximated at high accuracy. This is essential for assessing volume-based diagnostic parameters, like EF. Concerning shape conformity we can see that a high overlap between the two shapes is achieved, although the VOD is still improvable. The distance metrics d_{min} and d_{ortho} are near the mean reconstruction error of 2.3 mm [11].

Sim. Metric	Mean	Std.	Min.	Max.
d_{min} (mm)	2.61	0.65	1.65	3.53
d_{ortho} (mm)	2.49	0.77	1.38	3.72
DOV (%)	94.56	3.55	87.35	98.73
VOD (%)	78.17	5.30	68.88	84.91
κ (%)	87.12	2.53	82.54	90.18

Table 1. Evaluation of LV shape recovery from simulated angiograms.

4.3. Evaluation based on Real Patient Data

For three patients, a corresponding CT image is available for the RAO/LAO in-vivo angiograms. Note that this allows an accurate evaluation of our approach since the true 3-D LV shape is exactly known from CT. Evaluation based on the three in-vivo angiograms is performed as follows: 1) a SSM is learned from 19 of the 20 data sets, with the CT data set corresponding to the angiograms being excluded, 2) the model is fit to interpolated angiographic RAO/LAO frames of a single cardiac cycle showing the LV at 65% of the heart phase, and 3) the recovered shape is compared with the true 3-D shape of the excluded CT data set using the defined similarity metrics. The angiograms are acquired using a Siemens Bicor and a Siemens AXIOM Artis dBC system, capturing images of 512×512 pixels and 8-bit gray level depth at a frame-rate of 25 fps. For temporal registration with CT data in step 2, the ECG information accompanying the angiograms is utilized. The results for three in-vivo angiograms are given in Tab. 2. Our experiments indicate that values similar to the evaluation with simulated data are achieved, although the number of data sets is relatively small. The best shape conformity is achieved for example #2. For example #3, the reconstruction yields suboptimal results.

Sim. Metric	#1	#2	#3	Mean	Std.
d_{min} (mm)	2.43	2.32	2.95	2.57	0.34
d_{ortho} (mm)	2.36	2.05	3.36	2.59	0.68
DOV (%)	98.01	92.87	82.11	91.00	8.11
VOD (%)	74.72	80.13	68.12	74.32	6.01
κ (%)	87.49	90.41	79.75	85.88	5.51

Table 2. Evaluation of LV shape recovery from three in-vivo angiograms.

5. Discussion and Conclusion

In this work, a new method for recovering the LV from contrast-enhanced bi-planar cine-angiographic x-ray images has been proposed. The novelty of our approach is that a-priori information about the LV anatomy is learned from high-resolution CT images, modeled as a SSM and utilized for reconstruction. A 2-D/3-D registration technique is applied to fit the SSM to angiographic projections.

When only two (noisy) projections are available, the reconstruction problem usually becomes underdetermined and ambiguous. In such cases, the incorporation of a-priori information plays an important role, since this can limit the space of possible solutions and improve the ability to deal with noisy data. In contrast to [7], anatomical a-priori information is derived from data of in-vivo instead of post-mortem subjects; other approaches often do not utilize this kind of information at all. Although only one bi-planar acquisition is used for reconstruction, our approach is generally not limited by the number of projections. However, since additional acquisitions increase the amount of radiation and bolus, this number is usually kept to a minimum.

Using a SSM for reconstruction allows to generate statistically plausible and patient specific shapes. Unlike other 3-D LV SSMs often found in literature, anatomical areas like the apex, the atrial concavity and the aortic valve region are preserved in our model. This is necessary to generate complete contour and densitometric information; otherwise, additional errors are introduced in the reconstruction process. Further note that these areas typically overlap with the ventricular cavity in projection images and are therefore hard to recover without prior knowledge.

Evaluation with both simulated data and real patient data shows promising results. The LV volume is recovered at high accuracy. This is important for assessing volumetric diagnosis parameters, like EF. Concerning shape conformity, the overlap between original and recovered volume is high, though there is still place for minor improvements. Future work will focus on improving the model fitting process and on evaluating our approach with more in-vivo angiograms.

References

[1] S. Benameur, M. Mignotte, S. Parent, H. Labelle, W. Skalli, and J. de Guise. 3D/2D Registration and Segmentation of Scoliotic Vertebrae using Statistical Models. *Computerized Medical Imaging and Graphics*, 27:321–337, 2003.

[2] T. F. Cootes, C. J. Taylor, D. H. Cooper, and J. Graham. Active Shape Models - Their Training and Application. *Computer Vision and Image Understanding*, 61:38–59, 1995.

[3] G. T. Herman and A. Kuba. Discrete Tomography in Medical Imaging. *Proceedings of the IEEE*, 91:1612–1626, 2003.

[4] H. Lamecker, T. H. Wenckebach, and H.-C. Hege. Atlas-Based 3D-Shape Reconstruction from X-Ray Images. In *ICPR '06: Proceedings of the 18th International Conference on Pattern Recognition*, pages 371–374. IEEE Computer Society, 2006.

[5] R. Medina, M. Garreau, J. Toro, H.L. Breton, J.-L. Coatrieux, and D. Jugo. Markov Random Field Modeling for Three-Dimensional Reconstruction of the Left Ventricle in Cardiac Angiography. *IEEE Transactions on Medical Imaging*, 25:1087–1100, 2006.

[6] M. Moriyama, Y. Sato, H. Naito, M. Hanayama, T. Ueguchi, T. Harada, F. Yoshimoto, and S. Tamura. Reconstruction of Time-Varying 3-D Left-Ventricular Shape from Multiview X-Ray Cineangiocardiograms. *IEEE Transactions on Medical Imaging*, 21:773–785, 2002.

[7] G. P. M. Prause and D. G. W. Onnasch. Binary Reconstruction of the Heart Chambers from Biplane Angiographic Image Sequences. *IEEE Transactions on Medical Imaging*, 15:532–546, 1996.

[8] M. Prummer, J. Hornegger, G. Lauritsch, L. Wigstrom, E. Girard-Hughes, and R. Fahrig. Cardiac C-Arm CT: A Unified Framework for Motion Estimation and Dynamic CT. *IEEE Transactions on Medical Imaging*, 28:1836–1849, 2009.

[9] J. Rieber, C. Rohkohl, G. Lauritsch, H. Rittger, and O. Meissner. Application of C-Arm Computed Tomography in Cardiology. *Der Radiologe*, 49:862–867, 2009.

[10] R. Swoboda, M. Carpella, W. Backfrieder, C. Steinwender, C. Gabriel, and F. Leisch. From 2D to 4D in Quantitative Left Ventricle Wall Motion Analysis of Biplanar X-Ray Angiograms. In *Computers in Cardiology 2005*, pages 977–980. IEEE Computer Society Press, 2005.

[11] R. Swoboda and J. Scharinger. A 3-D Statistical Shape Model of the Left Ventricle - Geometric Prior Information for Recovering Shape from Projective Bi-Planar X-Ray Images. In *Challenges in Biosciences: Image Analysis and Pattern Recognition Aspects*, pages 53–62. books@ocg.at, 2008.

[12] R. Swoboda, J. Scharinger, and C. Steinwender. Model-Based 3-D LV Shape Recovery in Biplane X-Ray Angiography: A-Priori Information Learned from CT. In *2015 Computing in Cardiology Conference (CinC)*, pages 101–104, 2015.